Progress In Electromagnetics Research Letters, Vol. 74, 47–52, 2018

Frequency Tunable Low-Cost Microwave Absorber for EMI/EMC Application

Gobinda Sen* **and Santanu Das**

Abstract—A frequency tunable multi-layer low cost microwave absorber is proposed for Ku and X bands of applications. The tunability is obtained with the cavity model design using two metallic layers; a frequency selective surface (FSS) layer and a metal backed substrate layer with the air gap between them. The change in air-gap results in variation of the effective substrate height, and as a consequence the resonant frequency is tuned. The coupling of LC resonance and cavity resonance at an air-gap of 7.5 mm results in a dual-band absorption of the design. The proposed absorber performance has been analyzed for both TE and TM polarizations of incident wave, and the results are found to be same. The studies on surface current distribution and incident angle variation are observed to get physical insight behind absorption. The waveguide measurement method is used to correlate the simulated results with the measured one. With this simple cost-efficient design, the absorber appears well suited for microwave application at X and Ku bands.

1. INTRODUCTION

Over the past decade, since the first 'perfect' metamaterial absorber (PMA) was proposed by Landy et al. [1], the microwave community has started to show a growing interest in it. Their PMA structure consisted of three layers (two metallic layers and a dielectric spacer). The strong coupling of the incident electric field at the top layer (electric ring resonator 'ERR') together with the ground metallic plane produced electric resonance at resonance frequency. The anti-parallel current induced from ERR causes magnetic resonance within the structure [2]. Following the work of Landy et al. numerous designs have been proposed for such absorbing components over a wide range of frequencies such as in the terahertz [3], infrared [4] and optical frequencies [5] for practical operations. Tunable metamaterial absorber has gained considerable attention owing to its flexible absorption frequency. In recent years, frequency reconfigurability has been achieved by changing some physical parameters [6], near-field interaction [7], and active elements, such as varactor diode or introducing lumped elements [8, 9] in the design. Single band to dual band absorption is obtained by changing air-gap between two metallic layers [10]. However, all the above techniques have certain limitations with respect to design cost, low profile, biasing network, polarization insensitiveness and fabrication challenges.

In the proposed design of the microwave absorber, the frequency shifting in single band is achieved with air-gap variation between the two metallic layers. Two layers of substrate with simple unit cell geometry is placed one after another while maintaining the air-gap between them. The variation of the air-gap or the cavity height makes the design frequency tunable with more than 95% absorption in the operation band of frequencies. The polarization insensitivity to the TE and TM incident wave makes the structure efficient in practical environment. The simulated and measured results obtained by waveguide measurement method are found similar.

Received 6 December 2017, Accepted 6 March 2018, Scheduled 20 March 2018

* Corresponding author: Gobinda Sen (gobinda.dets@gmail.com).

The authors are with the Department of Electronics and Telecomm. Engineering, Indian Institute of Engineering Science and Technology, Shibpur, Howrah, India.

2. ABSORBER DESIGN

The proposed absorber comprises an array of unit cells arranged periodically. Unit cell dimensions of the proposed tunable absorber are shown in Fig. 1. The structure is developed on two layers of an FR-4 Epoxy substrate (dielectric constant = 4.4, loss tangent = 0.02) of thickness 1.5 mm. The top layer unit cell consists of one square metallic ring loaded with arrow shape slot diagonally placed above the substrate, and the bottom layer includes a metal backed substrate as shown in Fig. 1. The analysis is carried out using CST Microwave Studio, and the corresponding results are given in the next section. The design parameters of the tunable metamaterial inspired absorber as shown in Fig. 1 are given in Table 1. The air gap (G) is varied to obtain tuning of the absorption band of the component. For adjustment of the air gap (G), the upper FSS layer is placed above the grounded substrate layer with the help of four adjustable screws.

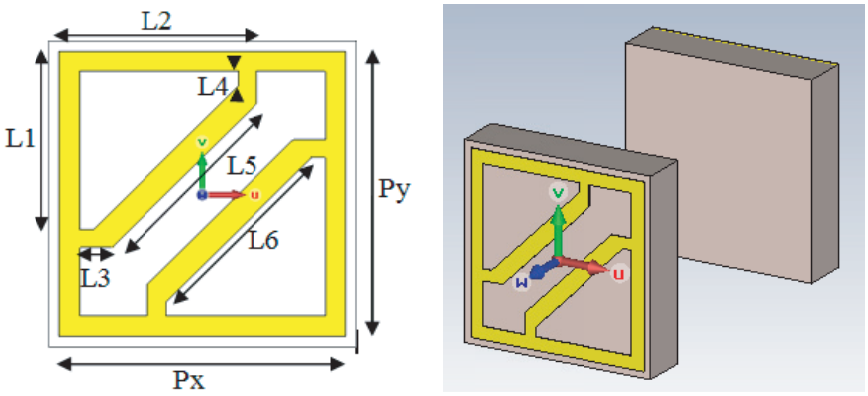

Figure 1. (a) The unit cell dimensions FSS layer. (b) The prospective design view of the proposed absorber.

Table 1. Designed dimensions (in mm) of the proposed structure.

Px	Py	$L1$	$L2$	$L3$	$L4$	$L5$	$L6$
8	6.3	0.8	9.5	0.6	3.3	0.2	0.2

3. ANALYSIS & SIMULATION

Due to complex permittivity and permeability of metamaterials absorbers, the absorbed EM power is modeled as the amount of loss experienced in the structure [11], characterized by,

$$A(w) = 1 - R(w) - T(w) \tag{1}$$

where, $R(w)$ and $T(w)$ are the frequency dependent functions for reflection and transmission coefficients of the component. The selection of the metal-backed substrate ensures the transmission coefficient becoming a zero, and hence Equation (1) is modified to give,

$$A(w) = 1 - R(w) \tag{2}$$

Therefore, to maximize absorption, the reflection coefficient is to be minimized as can be seen from the equations. To achieve it, the impedance of the structure is matched with the free space impedance.

From the view point of design, the structure can be considered as a rectangular cavity. The cavity walls are only bounded in the height by two layers; an FSS layer and a metal backed substrate. Fig. 2

illustrates a cavity model analogy of the design, and the corresponding resonant frequency, which is dependent on the cavity dimensions [12], is as given in Equation (3).

$$f_{nml} = \frac{ck_{nml}}{2\Pi} = \frac{c}{2}\sqrt{[(l/Py)^2 + (m/G_t)^2 + (n/Px)^2]} \tag{3}$$

where, k and c are the wave number and velocity of light, respectively. G_t is the total gap between the metallic layers. n, m, l are indicating the mode numbers. With the increasing air gap between two layers, the absorption frequency shifts to lower band as observed from Fig. 3 and justified with Equation (3).

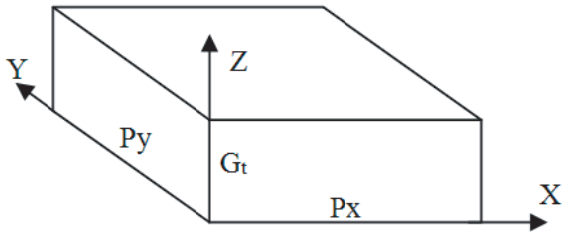

Figure 2. Cavity model analysis of the proposed design.

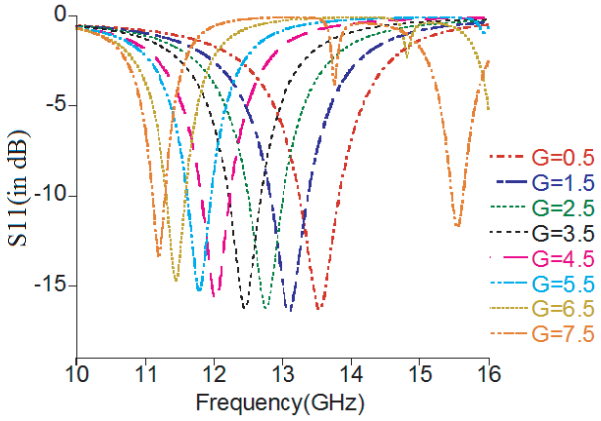

Figure 3. The reflection coefficient (S_{11} in dB) performance with air-gap ('G' in mm).

The simulated reflection coefficients S_{11} (dB) of the absorber for both the TE/TM polarizations are plotted in Fig. 3, which shows that the results are superimposed for the two polarizations. The parametric studies on the air-gap separation ('G' in mm) as depicted in Fig. 3 show tunability performance of the structure. The contributions of different resonances like LC resonance and cavity resonance to absorption of incoming wave are analyzed using surface current distribution on the structure due to induced fields.

Figures 4–6 show the surface current distributions on the top and bottom planes at the absorption frequency for the air-gaps (G) of 3.5 mm and 7.5 mm, respectively. The same analogy can be drawn for rest of the air-gap (G) variation. The surface current induced by the LC resonance is associated with the opposite current distribution at the vertical strip of the unit cell, and the patch current distribution is similar to that shown in Fig. 4 and Fig. 6. For the higher gap separation of 7.5 mm, another absorption peak comes at lower frequency due to cavity resonance. Fig. 5 shows the surface

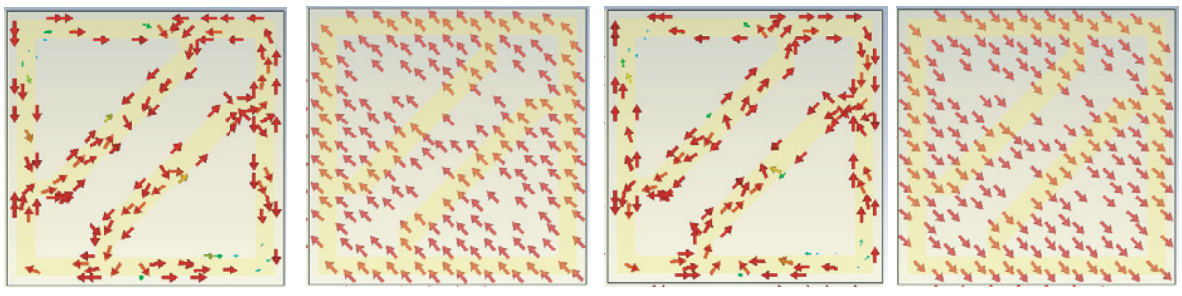

Figure 4. Surface current distribution on the (a), (c) top and (b), (d) bottom plane of the proposed absorber at the absorption peak of 12.46 GHz with airgap, $G = 3.5$ mm at (a), (b) TE, (c), (d) TM.

current at the absorption peak of 11.20 GHz which is uniformly distributed and parallel to each other at the two vertical strips of the unit cell. Coupling of the LC resonance and cavity resonance gives the dual-band absorption at 11.20 GHz and 15.56 GHz with higher air gap variation of 7.5 mm. The power loss density at the top surface of the unit cell is high at the diagonal edge of the arrow as compared to rest of the area as in Fig. 7.

The structure is also studied under varying angles of incidence of the incoming signal. A plot showing the absorptivity performances of the proposed structure is depicted in Fig. 8.

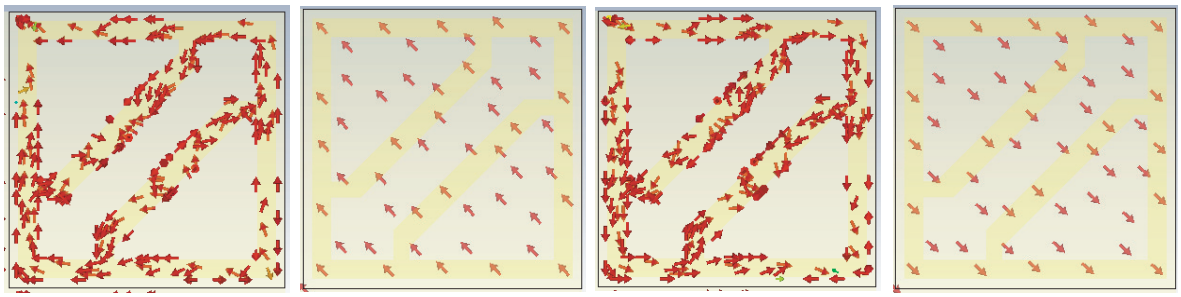

Figure 5. Surface current distribution on the (a), (c) top and (b), (d) bottom plane of the proposed absorber at the absorption peak of 11.20 GHz with airgap, $G = 7.5$ mm at (a), (b) TE, (c), (d) TM.

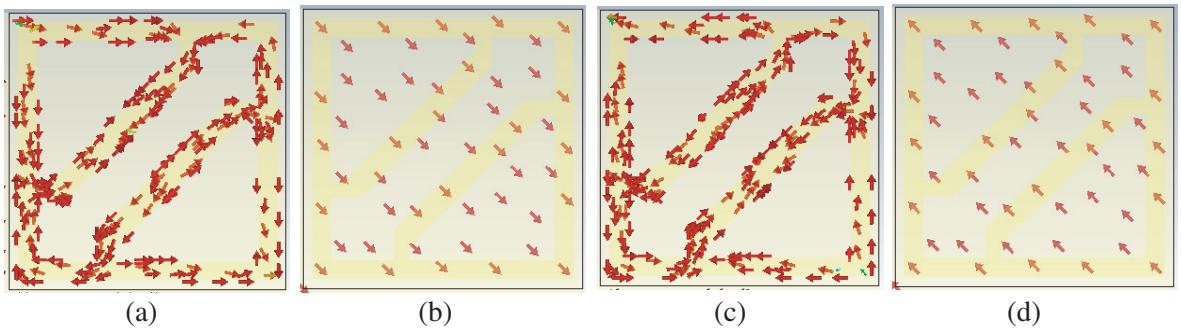

Figure 6. Surface current distribution on the (a), (c) top and (b), (d) bottom plane of the proposed absorber at the absorption peak of 15.56 GHz with airgap, $G = 7.5$ mm at (a), (b) TE, (c), (d) TM.

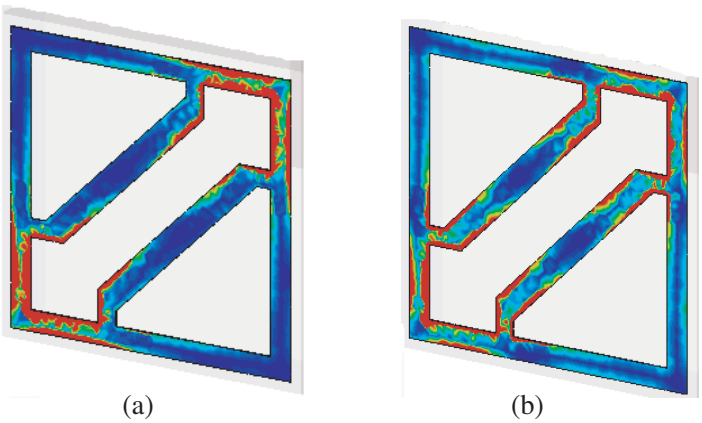

Figure 7. Surface power loss density at the top plane at the frequency of (a) 11.20 GHz, (b) 15.56 GHz for an air gap of 7.5 mm.

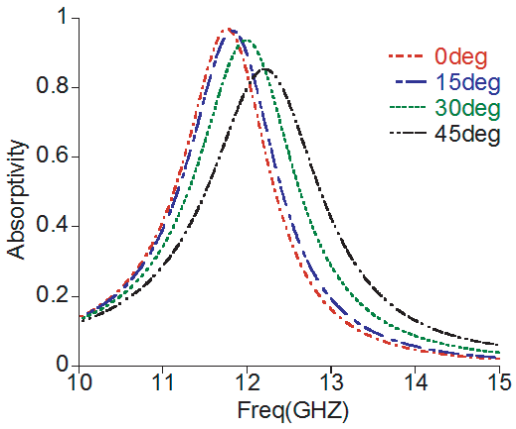

Figure 8. Absorptivity plot of the proposed one with incident angles.

4. EXPERIMENTAL RESULT

The proposed absorber is fabricated with standard PCB technology and shown in Fig. 9. The waveguide measurement method [13, 14] was used to test the absorption performance for its simplicity in measurement process. The proposed structure shows single absorption peak at 12.46 GHz for the lower height of 3.5 mm with double absorption peaks at 11.22 GHz and 15.54 GHz for higher gap of 7.5 mm. The electromagnetic waves come out from the waveguide and are incident on the interface of plane surface at an oblique angle of $\theta = \sin^{-1}(\lambda/2a)$ ('a' is the width of the aperture and λ the wavelength) [15]. The oblique incident angles for those resonance frequencies are calculated as 49.620, 35.850 and 37.650, respectively. A little discrepancy in the simulated and measured results is observed in Fig. 10, which may be due to imperfection in the manual air-gap separation, sensitivity to oblique incident angle and parallel placing of the two layers. Two standard waveguides operate in X and Ku bands, and an Agilent N5230A series Network Analyzer was used for the measurement process.

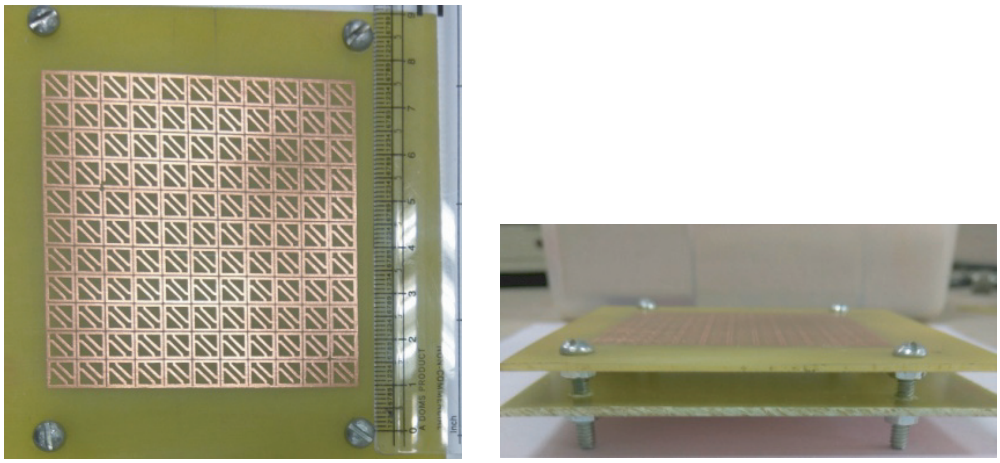

(a) (b)

Figure 9. Fabricated prototype of the absorber, (a) top view, (b) side view.

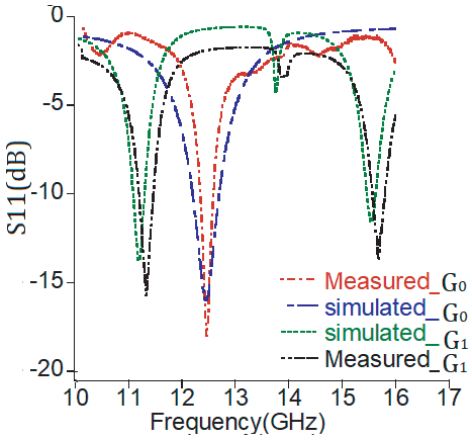

Figure 10. Simulated and measured reflection coefficient of the proposed absorber at $G_0 = 3.5$ mm, and $G_1 = 7.5$ mm.

5. CONCLUSION

A frequency tunable multilayer microwave absorber is designed in a cost-efficient way. With the use of easily adjusting screws, the air gap between two metallic layers is varied to obtain absorption peak at the desired frequency and henceforth eases the design fabrication and cost. The air gap (G) is varied from 0.5 mm to 7.5 mm to obtain absorption peak in the X and Ku bands. At higher air gap separation, the single absorption band shifts downward due to increase in effective substrate height. The coupling between LC and cavity resonance results in dual-band performance of the absorber at the higher gap of 7.5 mm. Thus, the design is able to tune absorption frequency without using any active element in the structure, therefore may be useful for applications such as radar cross section and electromagnetic interference (EMI) reduction.

REFERENCES

1. Landy, N. I., S. Sajuyigbe, J. J. Mock, D. R. Smith, and W. J. Padilla, "Perfect metamaterial absorber," *Physical Review Letters*, Vol. 100, No. 20, 207402, 2008.
2. Rufangura, P. and C. Sabah, "Polarisation insensitive tunable metamaterial perfect absorber for solar cells applications," *IET Optoelectronics*, Vol. 10, No. 6, 12, 2016.
3. Grant, J., et al., "Polarization-insensitive terahertz metamaterial absorber," *Opt. Lett.*, Vol. 36, No. 8, April 2011.
4. Zhu, W. and X. Zhao, "Metamaterial absorber with dendritic cells at infrared frequencies," *J. Opt. Soc. Amer. B*, Vol. 26, No. 26, 2382–2385, December 2009.
5. Gong, Y., et al., "Highly flexible all-optical metamaterial absorption switching assisted by Kerr-nonlinear effect," *Opt. Express*, Vol. 19, No. 11, 10193–10198, 2011.
6. Zhai, H., et al., "A new tunable dual-band metamaterial absorber with wide-angle TE and TM polarization stability," *Journal of Electromagnetic Waves and Applications*, Vol. 29, No. 6, 774–785, 2015.
7. Wang, B. X., L. L. Wang, G. Z. Wang, W. Q. Huang, X. F. Li, and X. Zhai, "Frequency continuous tunable terahertz metamaterial absorber," *J. Lighwave Technol.*, Vol. 32, 1183–1189, 2014.
8. Zhao, J., Q. Cheng, J. Chen, M. Q. Qi, W. X. Jiang, and T. J. Cui, "A tunable metamaterial absorber using varactor diodes," *New J. Phys.*, Vol. 15, 043049, 2013.
9. Lin, B. Q., S. H. Zhao, W. Wei, X. Y. Da, Q. R. Zheng, H. Y. Zhang, and M. Zhu, "Design of a tunable frequency selective surface absorber as a loaded receiving antenna array," *Chin. Phys. B*, Vol. 23, 024201, 2014.
10. Zheng, H. Y., X. R. Jin, J. W. Park, Y. H. Lu, J. Y. Rhee, W. H. Jang, H. Cheong, and Y. P. Lee, "Tunable dual-band perfect absorbers based on extraordinary optical transmission and Fabry-Perot cavity resonance," *Opt. Express*, Vol. 20, 24002–24009, 2012.
11. Chen, J., Z. Hu, G. Wang, X. Huang, S. Wang, X. Hu, and M. Liu, "High-impedance surface-based broadband absorbers with interference theory," *IEEE Transactions on Antennas and Propagation*, Vol. 63, No. 10, 4367–4374, October 2015.
12. Collin, R. E., *Foundations for Microwave Engineering*, 501, 2nd Edition, Wiley-IEEE Press, January 2001.
13. Zhai, H., C. Zhan, L. Liu, and Y. Zang, "Reconfigurable wideband metamaterial absorber with wide angle and polarization stability," *Electronics Letters*, Vol. 51, No. 21, 1624–1626, October 8, 2015.
14. You, J. W., J. F. Zhang, W. X. Jiang, H. F. Ma, W. Z. Cui, and T. J. Cui, "Accurate analysis of finite-volume lumped elements in metamaterial absorber design," *IEEE Transactions on Microwave Theory and Techniques*, Vol. 64, No. 7, 1966–1975, July 2016.
15. Li, L., Y. Yang, and C. H. Liang, "A wide-angle polarization insensitive ultra-thin metamaterial absorber with three resonant modes," *J. Appl. Phys.*, Vol. 110, 063702, 2011.